

Stereo Rectification for Equirectangular Images

Akira Ohashi,^{1,2} Fumito Yamano,¹ Gakuto Masuyama,¹ Kazunori Umeda,¹
Daisuke Fukuda,² Kota Irie,³ Shuzo Kaneko,² Junya Murayama,² and Yoshitaka Uchida²

Abstract—This paper proposes a method of stereo rectification for stereo camera using two fisheye cameras. Rectification parameters are estimated from feature points obtained from an image of an arbitrary environment. Errors due to deviation of the position and rotation of the left and right cameras are removed by stereo rectification. The performance of the fisheye stereo camera using equirectangular images is evaluated by simulation and experiments. It is shown that accuracy of range measurement is improved by the proposed rectification.

I. INTRODUCTION

In recent years, increasing numbers of cameras and range sensors have been installed in vehicles to assist with driving. Since the cost is proportional to the quantity of sensors, it is important for sensors to capture a wide range of environmental information. In this paper, we focus on a fisheye camera. The fisheye camera has a view angle of 180 degrees or more, and its size is relatively small. Therefore, the fisheye camera is easily installed in a vehicle or robot. Several studies have been conducted regarding the use of fisheye cameras in vehicles, regarding subjects such as lane detection [1], the estimation of vehicle pose [2], and obstacle detection [3]. In some studies, a driver assistance system has been constructed using multiple fisheye cameras [4][5]. An overhead view of the entire circumference is created from multiple camera images. A fisheye stereo camera can be constructed by using two fisheye cameras. Abraham et al. [6] simplified stereo matching by rectifying the images of the fisheye stereo camera. Moreau et al. [7] discussed the epipolar constraint of fisheye image for equisolid angle projection model and achieved environmental restoration using a stereo camera. However, the method has large computational costs. Hane et al. [8] achieved real-time three-dimensional measurement by using the plane-sweeping method. In some studies, a fisheye stereo camera was applied to a practical platform such as UAV [9] and vehicles [10][11][12]. In these studies, fisheye images were usually transformed to perspective images to simplify the corresponding point search of stereo images. With this, the peripheral regions of the image are severely stretched. Consequently, it becomes difficult to carry out stereo matching at the peripheral regions, and the detection range of the distance becomes narrower than when images that are not deformed by a fisheye are used. Therefore, we proposed a fisheye stereo camera that uses equirectangular

projection as a method of solving image stretching [13]. Equirectangular projection can convert fisheye images into images in which the vertical axis and the horizontal axis of the rectangular coordinate system are the latitude and longitude on the hemisphere of the fisheye lens. Equirectangular projection simplifies the corresponding point search without severely stretching the peripheral region. However, the accuracy of the proposed image correction is low, the accuracy of the distance measurement is not high, and correction parameters cannot be updated during distance measurement. In this paper, to update the correction parameters while measuring distance, stereo images are rectified by using feature points in an equirectangular image captured in an arbitrary environment. We evaluate the proposed wide-range measurement method by comparing it to a fisheye stereo camera that uses perspective projection.

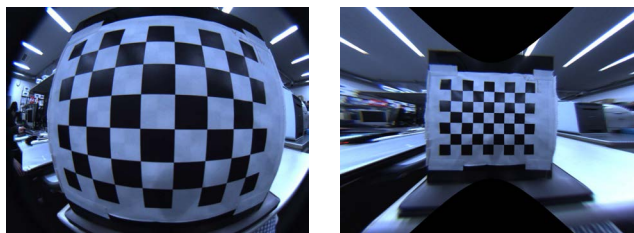
II. THE FISHEYE STEREO CAMERA

A. Fisheye Camera Model [14]

Many fisheye lenses use an equidistant projection, which is the projection model of the distance of the center of the image proportional to an angle. In addition to equidistant projection, there are other projection methods, such as orthogonal projection, stereographic projection, and equisolid angle projection. However, an actual fisheye camera does not follow these ideal projection models exactly. In this paper, internal parameters are calculated by using the camera model proposed by Scaramuzza et al. [14], and the influence due to individual difference of the camera is corrected by equirectangular projection.

B. Equirectangular Projection

As shown in Fig. 1, when perspective projection is applied to a fisheye image, the center region of the image is smaller, and the peripheral regions of the image are stretched. Since image quality in the reduced center region and the stretched



(a) Fisheye image

(b) Perspective image

Fig. 1. Comparison of a fisheye image and a perspective image

¹The Course of Precision Engineering, School of Science and Engineering, Chuo University, Tokyo, Japan
yamano@sensor.mech.chuo-u.ac.jp

² Clarion, Saitama, Japan

³ Hitachi Automotive Systems Americas, Inc., 34500 Grand River Ave., Farmington Hills, MI, 48335, USA

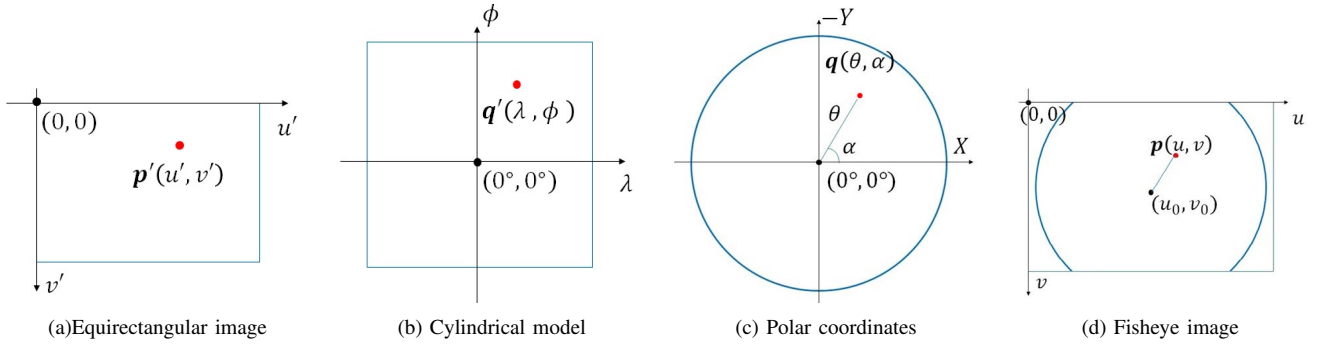


Fig. 2. Process of generating an equirectangular image

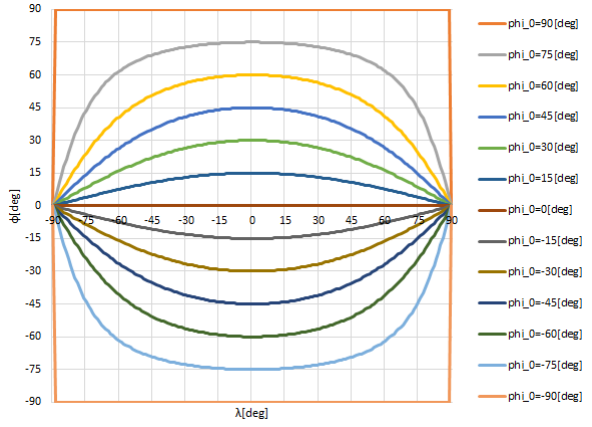


Fig. 3. Epipolar lines on an equirectangular image

peripheral regions is bad, it is difficult to obtain corresponding points in these regions by stereo matching. Therefore, to remove the distortion of the fisheye image and decrease the stretching of the image caused by projection, equirectangular projection is applied to the fisheye image. Since equirectangular projection can change the fisheye image into an image vertically equidistant, which has low distortion, and keep the form of the image, the images with equirectangular projection can be easily searched for stereo correspondence. The process of the equirectangular projection is described below.

- 1) The target pixel position of the equirectangular image p' , as shown in Fig. 2(a), is projected into the pixel position of the cylindrical model q' , as shown in Fig. 2(b).
- 2) The pixel position of the cylindrical model q' , as shown in Fig. 2(b), is projected into the pixel position of polar coordinate q , as shown in Fig. 2(c).
- 3) By using the internal parameters of the camera, the pixel position of polar coordinate q as shown in Fig. 2(c), is projected into the pixel position of the fisheye image p as shown in Fig. 2(d).

- 4) The pixel value of the pixel position of the equirectangular image p is inserted into the target pixel position of the equirectangular image p' .

C. Corresponding Point Search for Equirectangular Image

In this paper, template matching is used to search corresponding points. The sum of absolute differences (SAD) in brightness is used as the similarity. The elevation angle ϕ , when azimuth angle $\lambda = 0$, is ϕ_0 ; epipolar lines of equirectangular images can be expressed as (1).

$$\phi = \tan^{-1}(\tan \phi_0 \cos \lambda) \quad (1)$$

The trajectory of ϕ when ϕ_0 of this equation is fixed at ± 90 [°], ± 75 [°], ± 60 [°], ± 45 [°], ± 30 [°], ± 15 [°], 0 [°] are shown in Fig. 3; in other words, Fig. 3 shows epipolar lines on an equirectangular image. The horizontal axis and the vertical axis in Fig. 3 correspond to the azimuth angle and the elevation angle, respectively, of the fisheye stereo camera. When applying template matching to equirectangular images, corresponding points are searched for on the epipolar line.

D. Distance Measurement Method for Equirectangular Image

When the baseline length is b , the disparity of azimuth angle is $\Delta\lambda$, the azimuth angle between left camera and measurement target is λ_l , the elevation angle between right camera and measurement target is ϕ_r , the Euclidean distance between the camera and the object D (note: not the distance in the direction of the optical axis, hereinafter simply referred to as distance) is expressed as the next equation:

$$Z = \frac{b}{\sin \Delta\lambda} \frac{\cos \lambda_l}{\cos \phi_r} \quad (2)$$

From (2), we see that with the stereo camera, measurement accuracy in the horizontal direction is better when the cameras are placed side by side vertically than when the cameras are placed side by side horizontally. However, installing cameras side by side vertically is difficult in vehicles. Therefore, for this paper, we placed cameras side by side horizontally.

III. STEREO RECTIFICATION

A. Stereo Rectification for Perspective Images

Although many stereo cameras assume that the left and right cameras are completely parallel, errors are generated due to positional and postural deviations of the camera in real space. Therefore, it is necessary to remove the influence of the deviation by correcting the image that needs external parameters obtained from the estimation. To correct the deviation, a method called stereo rectification [15][16] has been proposed. When the postures of the left and right cameras are R_l and R_r , and the positions are T_l and T_r , the method of stereo rectification of the perspective image is shown below.

- 1) Estimate a essential matrix of the cameras by a 5-point algorithm [17].
- 2) Calculate R_l , T_l from the essential matrix.
- 3) Calculate R_{rect} from eqs. (3) to (8) ($R_r = I$ (identity matrix), $T_r = 0$).

$$R = R_l^T \quad (3)$$

$$T = T_l \quad (4)$$

$$e_1 = \frac{T}{\|T\|} \quad (5)$$

$$e_2 = \frac{T}{\sqrt{T_x^2 + T_y^2}} [-T_y \ T_x \ 0]^T \quad (6)$$

$$e_3 = e_1 \times e_2 \quad (7)$$

$$R_{rect} = \begin{pmatrix} e_1^T \\ e_2^T \\ e_3^T \end{pmatrix} \quad (8)$$

- 4) Multiply the left image and $R_{rect}R$, the right image and R_{rect} .

Therefore, the left image and the right image are rectified, and the epipolar lines become horizontal straight lines.

B. Stereo Rectification for Equirectangular Images

To apply the method of stereo rectification outlined in Section III-A to the equirectangular image, the coordinate of the equirectangular image is converted to the coordinates of the perspective image. Then, the points in the perspective image are rectified and converted to the points in the equirectangular image. The transformation equation and the inverse transformation equation for the coordinates of the equirectangular image (λ, ϕ) to the coordinates of the perspective image (x, y, z) are shown in equations (9) and (10).

$$\begin{pmatrix} x \\ y \\ z \end{pmatrix} = \begin{pmatrix} \tan \lambda \\ \frac{\tan \phi}{\cos \lambda} \\ 1 \end{pmatrix} \quad (9)$$

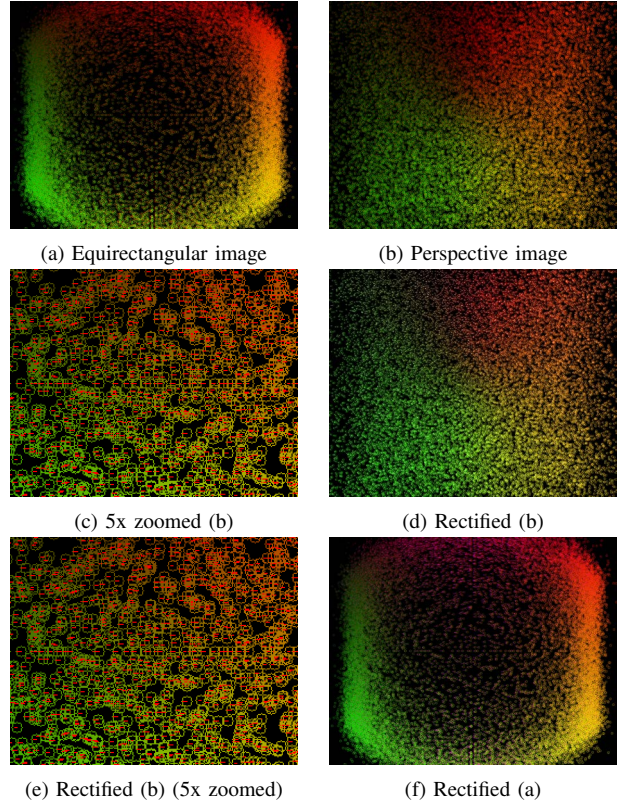


Fig. 4. Rectification in condition 1

$$\begin{pmatrix} \lambda \\ \phi \end{pmatrix} = \begin{pmatrix} \arctan x \\ \arctan \frac{y}{\sqrt{1+x^2}} \end{pmatrix} \quad (10)$$

TABLE I
ESTIMATED ERROR OF ROTATION AMOUNT AND TRANSLATIONAL
AMOUNT OF LEFT CAMERA

	true value	estimation value	error[%]
roll [°]	5	4.983	0.340
pitch [°]	5	4.977	0.460
yaw [°]	5	5.055	1.100
y [mm]	1	1.080	8.000
z [mm]	-1	-1.050	5.000

IV. SIMULATION OF STEREO RECTIFICATION

In order to evaluate the accuracy of external parameter estimation and the accuracy of image correction in III-A and III-B, the method of stereo rectification is simulated by virtual three-dimensional points in equirectangular image.

A. Simulation Conditions

The baseline length of the fisheye stereo camera is 52 mm, and measurement objects are points in a range of 16 m horizontal (x), 16 m vertical (y), and 2 m ahead of the optical axis direction of the camera, and 25921 pairs of corresponding points in increments of 0.1 m in the x and y

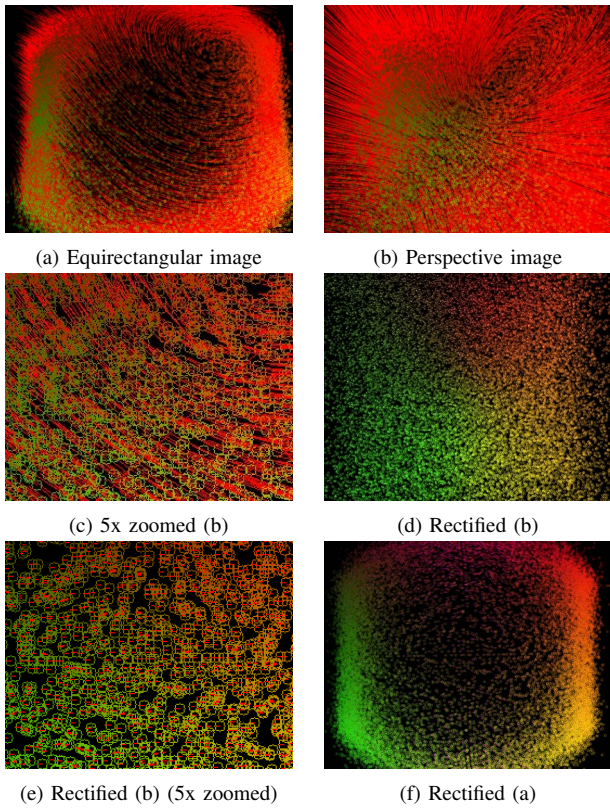


Fig. 5. Rectification in condition 2

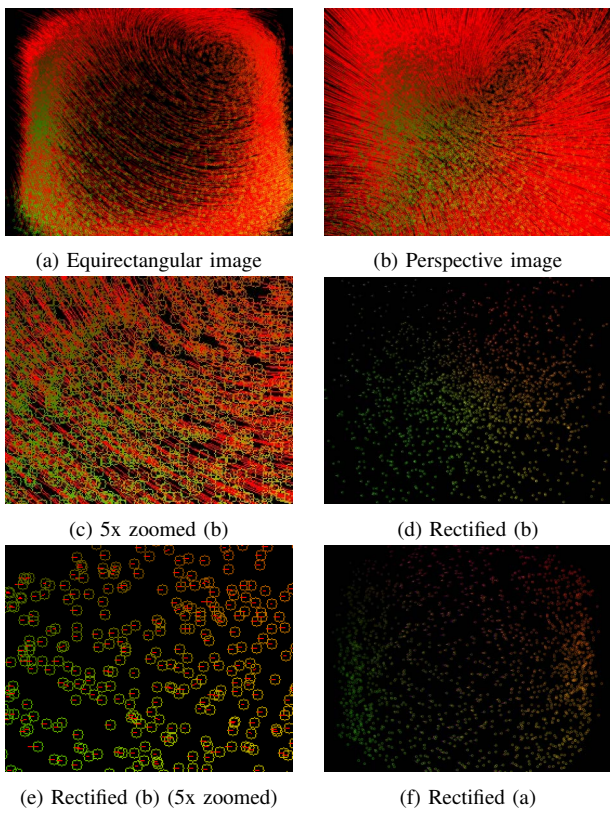


Fig. 6. Rectification in condition 3



Fig. 7. Fisheye images captured in the experimental environment

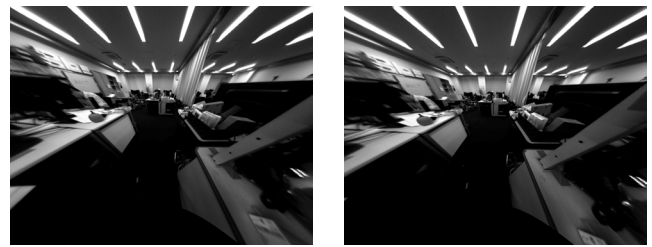


Fig. 8. Perspective images converted from Fig. 7



Fig. 9. Equirectangular images converted from Fig. 7

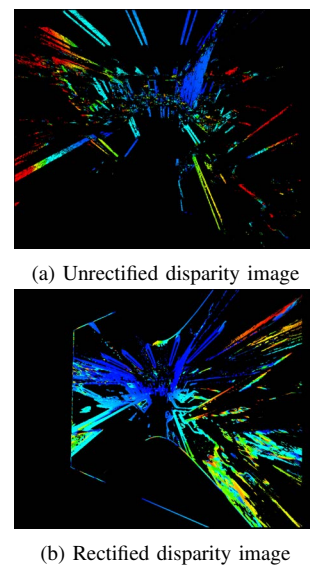
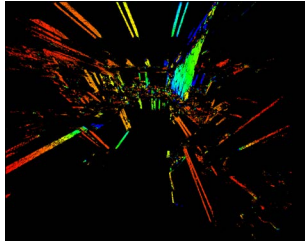
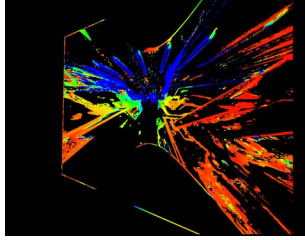


Fig. 10. Comparison of disparity image from Fig. 8

directions. Suppose that you can acquire a point. In addition, to stabilize the estimation of the translation component, the distance in the optical axis direction of each feature point

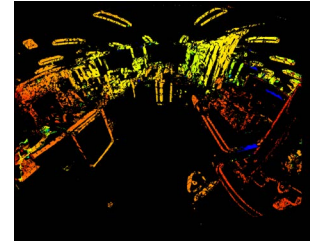


(a) Unrectified range image

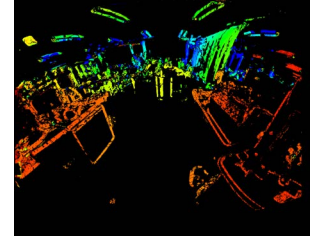


(b) Rectified range image

Fig. 11. Comparison of range image from Fig. 8

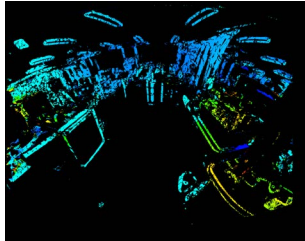


(a) Unrectified range image

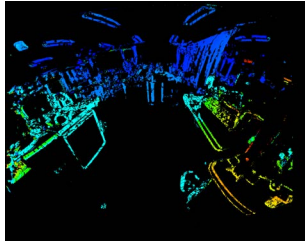


(b) Rectified range image

Fig. 13. Comparison of range image from Fig. 9



(a) Unrectified disparity image



(b) Rectified disparity image

Fig. 12. Comparison of disparity image from Fig. 9

is added to an average of 2 m and a standard deviation of 0.5 m, which is according to a normal distribution. The camera position and the posture of the right camera are fixed for no rotation and no translation. The camera position and the posture of the left camera are set with the following conditions.

- 1) No rotation and no movement.
- 2) Rotation of 5 degrees in x-, y-, and z-axis directions, and move 5 mm in the upper and backward directions.
- 3) In addition to condition 2, a standard deviation of 1.0 pixel is added in the u and v directions of the equirectangular image.

- 4) The pixel value of the pixel position of the equirectangular image p is inserted into the target pixel position of the equirectangular image p' .

In condition 3, RANSAC is applied to eliminate large dispersion points and improve the accuracy of the parameter estimation. The evaluation value of RANSAC is the deviation amount in the y direction between corresponding points on perspective coordinates. The threshold of RANSAC is 0.001, the number of RANSAC samples is 6, and the number of RANSAC loops is 10000.

B. Simulation Results

The results of conditions 1, 2, and 3 in the previous section are shown in Figs. 4, 5, and 6. To evaluate whether the disparity has been rectified, the central region of the perspective image is zoomed 5 times. In the simulation of condition 3, as a result of the final correction, 1900 points remain within the threshold of the evaluation value. These points are shown in Fig. 6 (d), (e), and (f). The red line shows disparity, the center of the colored circle shows the feature point on the left image, the edge of the red line on the side that does not have round is the feature point on the right image, the yellow line is the epipolar line extended from the feature point of the left image, and the purple line is the epipolar line extended from the feature point of the right image. Moreover, in the simulations of conditions 1 and 2, the estimation error is 0 at the rotation amount (roll, pitch, yaw, respectively) on the x, y, and z axes and the translation amount in the y direction and z direction. Table 1 shows the estimated parameters in the condition 3 simulation.

C. Discussion

Since the external parameters of conditions 1 and 2 are estimated without error and the parallax is horizontal in Figs. 4 (e) and 5 (e), rectification has succeeded in the simulations of conditions 1 and 2. Also, the estimation of the external

parameters in the simulation of condition 3 has some errors that are shown in Table 1. However, since the points in Fig. 6 (f) satisfy the threshold of the evaluation value and points are scattered throughout the image, rectification is considered to have succeeded.

V. STEREO RECTIFICATION EXPERIMENT

A. Experiment Conditions

As an experiment, range images are generated by using the proposed method as described above. The CMOS camera that we used was the Point Grey Research Flea3; the fisheye lens we used was the SPACE TV1634M. The number of pixels was 1328×1048 pixel, the pixel size was 3.63 m, the focal length of the lens was 1.6 mm, and the baseline length was 52 mm. The measurement range in the horizontal direction was $165 [^\circ]$, and the vertical direction was $132 [^\circ]$. Since it searches for corresponding points to the right during stereo matching, the measurement range in the horizontal direction is narrower than the horizontal angle of the camera's view. Intrinsic parameters of the fisheye camera were estimated by utilizing the OcamCalib Toolbox [14] in Matlab. The external parameters and the correction matrix of the left and right cameras were obtained by the proposed method. The estimation results of the left camera correction matrix R_L , and the right camera correction matrix R_R , are shown below.

$$R_L = \begin{pmatrix} 0.999 & -3.271 \times 10^{-2} & -2.462 \times 10^{-3} \\ 3.271 \times 10^{-2} & 0.999 & -5.725 \times 10^{-4} \\ 2.479 \times 10^{-3} & 4.917 \times 10^{-4} & 1.000 \end{pmatrix}$$

$$R_R = \begin{pmatrix} 1.000 & -1.980 \times 10^{-2} & -9.114 \times 10^{-3} \\ 1.980 \times 10^{-2} & 1.000 & -1.804 \times 10^{-4} \\ 9.116 \times 10^{-3} & 0.000 & 1.000 \end{pmatrix}$$

Since this estimation result shows that the correction matrix of each camera is close to the identity matrix, the positions of fisheye stereo cameras that is used in the experiment is almost parallel.

B. Experiment Result

Figure 7 is a fisheye image of the experimental environment taken with a fisheye stereo camera; the image in Fig. 8 is Fig. 7 converted by perspective projection. Figure 9 is the image from Fig. 7 converted by equirectangular projection. Figures 10 - 13 show the effects of rectification in disparity images and range images. In Figs. 10 - 13, the colors of red to blue correspond to 1 to 48 pixels, 0.5 to 10 m.

C. Discussion of Experiment Result

In comparing Figs. 10 - 13, when rectification is not applied, near object disparity and distance are measured as being similar to far object disparity and distance. However, when rectification is applied, the distance between near objects and far objects can be measured differently. It is thought that since the corresponding points have little disparity, much of the influence of the deviation was corrected by rectification. However, false matching occurs in the illuminated

regions on the images. This false matching is a problem that occurs in similar luminance patterns in the template during template matching; it is thought that in the future, it will be necessary to investigate the distance measurement results in regions with similar luminance patterns. Also, since the accuracy of specific distance measurement is unknown, quantitative evaluation is necessary.

VI. CONCLUSIONS

In this paper, we have incorporated stereo rectification using images captured in arbitrary environments into a wide-ranging distance measurement method. We have done this by applying a fisheye stereo camera using equirectangular images in a method of stereo rectification that uses images captured in arbitrary environments. This has allowed us to construct a fisheye stereo camera with correction parameters that can be updated during distance measurement. We aim to eliminate false matching and evaluate distance measurement accuracy.

REFERENCES

- [1] C. H. Kum et al., Lane detection system with around view monitoring for intelligent vehicle, Proc. of ISOCV, pp. 215-218, 2013.
- [2] S. Li et al., Estimating vehicle pose relative to current lane from fisheye camera system, Trans. on the IEEJ, vol. 131, no. 12, pp. 2189-2195, 2011.
- [3] C. T. Lin et al., A real-time rear obstacle detection system based on a fisheye camera, Proc. of APSIPA ASC, pp. 1-4, 2012.
- [4] T. Sato et al., Spatio-temporal bird's-eye view images using multiple fisheye cameras, Proc. of SII, pp. 753-758, 2013.
- [5] C. M. Huang et al., Fisheye cameras calibration for vehicle around view monitoring system, Proc. of ICCE-TW, pp. 225-226, 2014.
- [6] S. Abraham et al., Fisheye stereo calibration and epipolar rectification, Journal of ISPRS, vol. 59, no. 5, pp. 278-288, 2005.
- [7] J. Moreau et al., Equisolid fisheye stereovision calibration and point cloud computation, Proc. of ISPRS, vol. XL-7/W2, pp.167-172, 2013.
- [8] C. Hane et al., Real-time direct dense matching on fisheye images using plane-sweeping stereo, Proc. of 3DV, vol. 01, pp. 57-64, 2014.
- [9] N. Krombach et al., Evaluation of stereo algorithms for obstacle detection with fisheye lenses, Proc. of ISPRS, vol. II-1/W1, 2015.
- [10] P. Furgale et al., Toward automated driving in cities using close-to-market sensors: An overview of the V-Charge Project, Proc. of IEEE Intelligent Vehicles Symposium (IV), 2013.
- [11] S. K. Gehrig, Large-field-of-view stereo for automotive applications, Proc. of OmniVis, vol. 1, 2005.
- [12] D. Kim et al., Rear obstacle detection system with fisheye stereo camera using HCT, Journal of Expert Systems with Applications, vol. 42, no. 17, pp. 6295-6305, Oct. 2015.
- [13] A. Ohashi et al., Fisheye stereo camera using equirectangular images, Proc. of MECATRONICS-REM, 2016.
- [14] M. Ruffi et al., Automatic detection of checkerboards on blurred and distorted images, Proc. of IROS, pp. 3121-3126, Nice, France, September 2008.
- [15] A. Fusiello et al., A compact algorithm for rectification of stereo pairs, Proc. of Machine Vision and Applications, 2000.
- [16] R. I. Hartley, Theory and practice of projective rectification, Journal of Computer Vision, 1999.
- [17] D. Nister, An efficient solution to the five-point relative pose problem, Transactions on Pattern Analysis and Machine Intelligence, vol. 26, no. 6, pp. 756-777, 2004.